[1]Jinshan Yu

[2]Xizhe Zhang

[3]Longhuan Liu*

[3]Zhihong Fu

[4]Ning Li

[5]Chaopeng Luo*

[3]Xin Chen

Analysis of corrosion detection error of grounding grid under amplitude characterization

JES

Journal of Electrical Systems

Abstract: - Magnetic field amplitude detection is an important method for determining the positioning and corrosion degree of the grounding grid, and the conventional analysis only determines the grounding grid status by collecting single-component signals, which makes the diagnosis results of the grounding grid status susceptible to the influence of the collection process. By considering the single-component sensor device in the attitude deflection during the actual substation detection process, the analysis of the difference between the signals measured by the sensor under different attitude deflections is performed, and the degree of influence of the attitude deflection on the magnetic field amplitude characteristics is determined. Further, by analyzing the calculation error of the attitude angle on the corrosion degree of the ground grid, the correspondence between the sensor attitude and the calculation error of the corrosion degree was obtained. Finally, in order to reduce the influence of the sensor attitude on the detection signal, it is proposed that the detection scheme of measuring the three-component sensor signal and the attitude angle at the same time which could improve the accuracy of the detection system.

Keywords : Grounding Grid; Magnetic Field Amplitude; Sensor Attitude; Measurement Error

I. INTRODUCTION

Grounding grid is an important foundation to ensure the safe operation of the power system [1-3]. The grounding grid is always buried and underground, affected by the surrounding environment and corrosion, serious corrosion of the grounding grid will even produce a breakpoint, resulting in a reduction in the ability of the grounding grid to dissipate the current, and sometimes even produce an abnormal increase in the ground voltage and jeopardize the safety of the staff on inspection [4-8]. Therefore, it is necessary to evaluate the status of the grounding grid. Accurate detection of grounding grid topology and corrosion is an important basis for measuring the condition of the grounding grid [9, 10]. The surface magnetic field method, as a non-destructive testing method, generates a magnetic field at the surface of the ground by injecting and withdrawing electric current through the lead wires in the grounding grid so that current flows in the grid. The surface magnetic field is collected using a sensor device and the condition of the grounding grid is evaluated by analyzing the distribution of the surface magnetic field [11-13]. Zhang et al. [14, 15] analyzed the relationship between the variations of the three components Bx, By and Bz, determined the optimal excitation parameters by varying the frequency and amplitude of the excitation source and used a single horizontal component of the magnetic field Bx signal peak to localize the topology of the grounding grid.

*Corresponding author: Longhuan Liu, Chaopeng Luo

[1] Electric Power Research Institute of State Grid Tianjin Electric Power Company, Tianjin 300384, China;

[2] State Grid Tianjin Electric Power Company, Tianjin 300090, China;

[3] College of Electrical Engineering, Chongqing University, Chongqing 400044, China;

[4] State Grid Tianjin Electric Power Company High Voltage Branch, Tianjin, 300231, China;

[5] Science and Technology on Near-Surface Detection Laboratory, Wuxi, 214035, China.

In [16], the second-order or fourth-order calculation of the horizontal component magnetic field is carried out by the differential method to realize the intelligent identification of the topology of the grounding grid. Fu et al. [17] analyzed the Bz component for grounding grid topology localization in grounding grid detection and proposed wavelet edge detection for grounding grid topology identification with respect to the measurement characteristics of the dumb point method. Xie et al. [18] for the electromagnetic interference in the substation and weak electromagnetic signal extraction difficult problem, through the design of frequency selective amplifier circuit and trap, to avoid the influence of interference noise on the acquisition system, to achieve the acquisition of the weak magnetic field of the ground surface.

In the actual measurement process of grounding grid surface magnetic field, it is inevitable that there will be offset or jitter in the direction of the sensor to produce attitude deflection, so that the acquisition of the single-component magnetic field value is not exactly equivalent to the theoretical value and thus generating measurement errors, resulting in the existence of noise in the magnetic field signal, this kind of noise is different from the surrounding environment of the electromagnetic interference noise, which cannot be suppressed or rejected by means of circuit filtering in the later stage. In this paper, we characterize the deflection and jitter of the sensor measurement process by the attitude angle, calculated the magnetic field amplitude under different attitude angles, analyzed the influence of the attitude angle on the topology identification and corrosion calculation, and optimized the detection scheme to reduce the influence of the sensor attitude on the measurement results, to improve the accuracy of the state evaluation of the grounding grid.

II. GROUNDING GRID TOPOLOGY IDENTIFICATION ERROR

A. Calculation of surface magnetic field
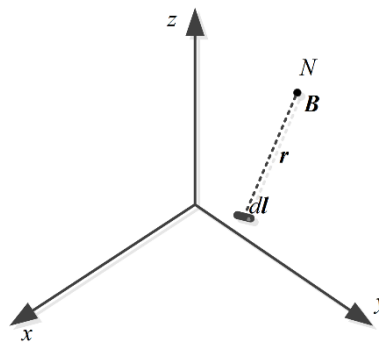
Fig. 1 Current-carrying conductor generates magnetic field in space

The size of substation grounding grid flat steel is generally 60mm × 8mm, grounding grid is generally greater than 3 m. The conductor itself is small in size relative to the grounding grid, ignoring the influence of the soil can be regarded as a number of long straight conductors constitute a pure resistance network. As shown in Figure 1 in the Cartesian coordinate system of any current for I conductor dl in the space point in the formation of the magnetic field dB, r for the distance between the two, the direction of the conductor pointing to the space point, μ0 for the magnetic permeability in a vacuum. By the Biot-Saval law has:

$$d\boldsymbol{B}(\boldsymbol{r}) = \frac{\mu_0}{4\pi} \frac{Id\boldsymbol{l} \times \boldsymbol{r}}{r^3} \qquad (1)$$

As shown in Figure 2 is a field type grounding grid model, the grid side length is 5m, the current is injected through point A and withdrawn at point C. The injected current size is 1A, L1 and L2 are two parallel measurement lines located at (y=2.5, z=0.8) and (y=7.5, z=0.8), respectively. Two types of data, Bx and $\partial Bz/\partial x$, were extracted from the survey line to be used as grounding grid topology extraction, and the curve of the data along the x-axis is shown in Fig. 3.
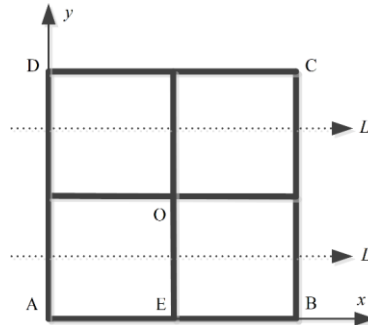
Fig.2 Top view of grounding grid model
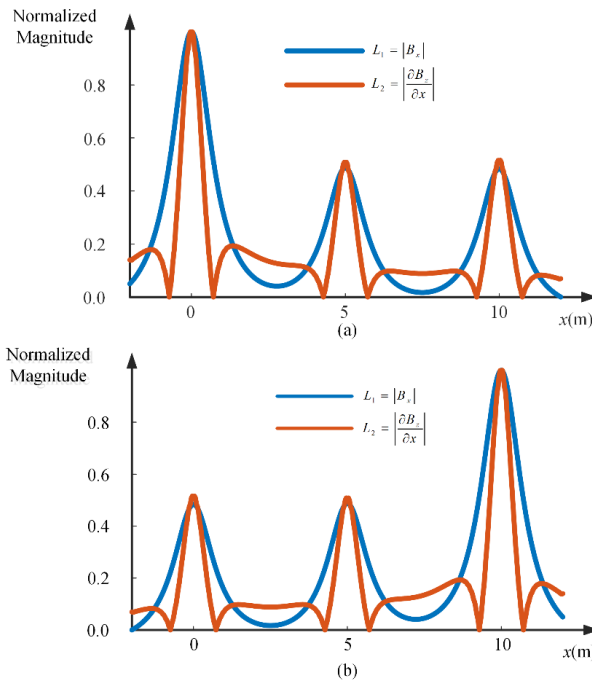
Fig.3 Peak and dummy point graphs

It can be noticed that at the positions of x=0.0m, x=5.0m and x=10.0m, the Bx magnetic field directly above the grounding grid reaches a localized peak, and the Bz magnetic field reaches a zero value and has the largest slope. Therefore, the grounding grid topology can be localized by the local peaks and local dummy points of the surface magnetic field.

B. Magnetic field calculation under sensor attitude deflection

In order to analyze the effect of sensor attitude on the measured magnetic field values, the magnetic field values received by the sensor in different attitudes need to be calculated. As shown in Fig. 4 in the Cartesian

coordinate system ex, ey and ez are the three direction vectors of the sensor in normal condition and ex', ey' and ez' are the three direction vectors after deflection.
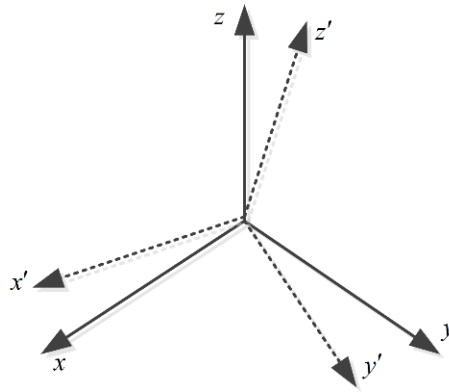
Fig.4 Attitude deflection schematic

The sensor is rotated around the x-axis, y-axis, and z-axis by a certain angle, respectively, and there are

$$\begin{bmatrix} e_{x'} \\ e_{y'} \\ e_{z'} \end{bmatrix} = \begin{bmatrix} 1 & 0 & 0 \\ 0 & \cos(\theta) & -\sin(\theta) \\ 0 & \sin(\theta) & \cos(\theta) \end{bmatrix} \begin{bmatrix} e_x \\ e_y \\ e_z \end{bmatrix} \tag{2}$$

$$\begin{bmatrix} e_{x'} \\ e_{y'} \\ e_{z'} \end{bmatrix} = \begin{bmatrix} \cos(\psi) & 0 & \sin(\psi) \\ 0 & 1 & 0 \\ -\sin(\psi) & 0 & \cos(\psi) \end{bmatrix} \begin{bmatrix} e_x \\ e_y \\ e_z \end{bmatrix} \tag{3}$$

$$\begin{bmatrix} e_{x'} \\ e_{y'} \\ e_{z'} \end{bmatrix} = \begin{bmatrix} \cos(\varphi) & -\sin(\varphi) & 0 \\ \sin(\varphi) & \cos(\varphi) & 0 \\ 0 & 0 & 1 \end{bmatrix} \begin{bmatrix} e_x \\ e_y \\ e_z \end{bmatrix} \tag{4}$$

where θ, ψ and φ are the angles of rotation of the sensor x-axis, y-axis and z-axis respectively. The magnetic field data that can be sensed by the sensor component at any attitude angle can be calculated by using Equation 2~4.

C.   *Effect of attitude angle on magnetic field eigenvalues*
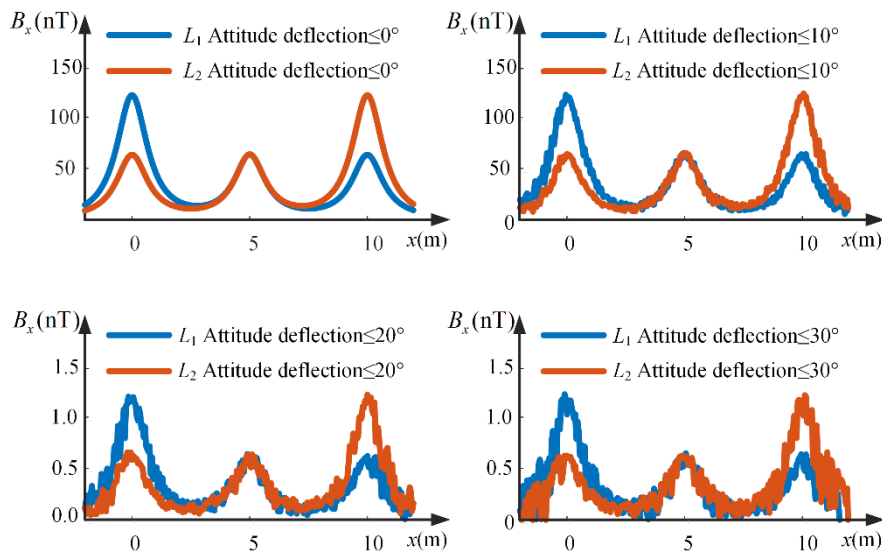
Fig. 5 Bx magnetic field values for different attitude deflections
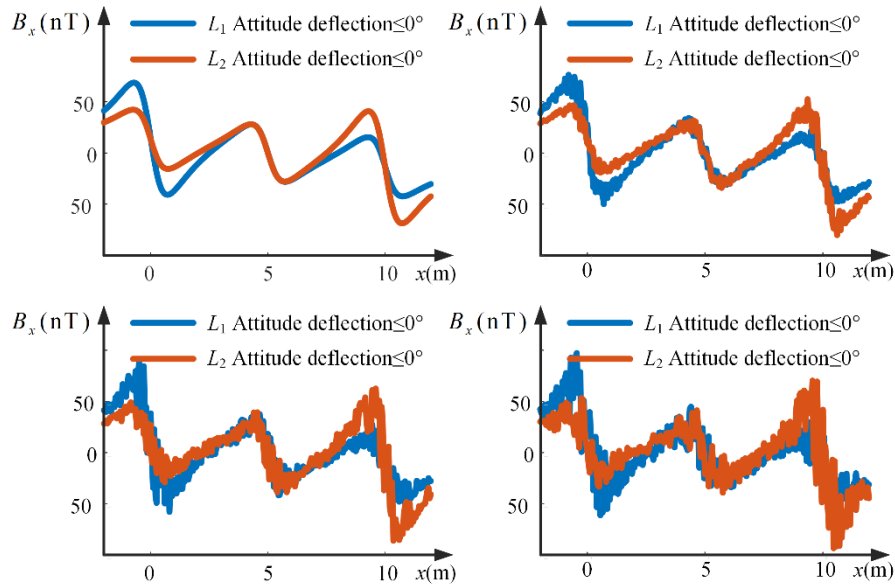
Fig. 6 Bz magnetic field values for different attitude deflections

As shown in Fig. 5 and Fig. 6 are the single component magnetic field strengths measured by the sensor along the measuring lines L1 and L2 when considering the maximum deflection angles of 0º, 10º, 20º and 30º, respectively. When the maximum deflection angle is 0º, there is no deflection in the sensor attitude at this time, and the Bx and Bz data are smooth directly above the grounding grid. When the deflection angle is not 0º, there is a certain angle of deflection of the sensor attitude, at this time, the magnetic field value obtained from the single-component measurement is the superposition of the three standard orthogonal components of the magnetic field value in a certain proportion, so that the measured value has a certain degree of noise compared to the magnetic field value without deflection, and the data noise will increase with the increase of the maximum deflection angle.

Passing a certain current right above the grounding grid will produce the maximum magnetic field value near the right above, so in the case of the same attitude deflection, the measurement error generated by the attitude of the sensor near the right above the grounding grid will be larger than other regions, which affects the localization of the local peak value or the maximum value of the local slope, and hence affects the accurate identification of the topology of the grounding grid.

III. GROUNDING GRID CORROSION CALCULATION ERROR

A. Signal strength at different degrees of corrosion

In order to analyze the effect of the sensor attitude on the sensitivity of corrosion detection, the signal strength of the grounding grid at different degrees of corrosion needs to be calculated. After injecting current into the grounding grid, the current will cause different current magnitudes to circulate in the corroded section according to the topology of the grounding grid and the corrosion of the flat steel, thus generating magnetic field differences at the ground surface. Flat steel corrosion is reflected in a thinner conductor structure, smaller cross-sectional area and increased conductor resistance. In a conductor of the same material and length, the resistivity expands by a factor of 1.2346 when the cross-sectional side length is reduced by a factor of 0.1 in

equal proportion. The surface magnetic field values are obtained by setting different corrosion degrees in the OE section in Fig. 2, and the signal values |Bx| and |∂Bz/∂x| at x=5.0 m are obtained by using the mean value method and the least squares method, respectively, to obtain the relationship of the signal strength with the corrosion degree as shown in Fig. 7.

For the signal value |Bx|, its signal strength decreases with increasing corrosion degree; for the signal value |∂Bz/∂x|, the signal value decreases with increasing corrosion degree between 0% and 80% of corrosion degree, and increases with increasing corrosion degree between 80% and 100% of corrosion degree. The reason for this phenomenon is that when the magnetic field Bx directly above the flat steel OE is mainly generated by the current circulating in the OE section, while ∂Bz/∂x is mainly affected by the OE section and other branches in the grid together, when the OE section due to corrosion leads to the current circulating at the same time, the other branches of the current is increased accordingly, so that |∂Bz/∂x | first decrease and then increase.
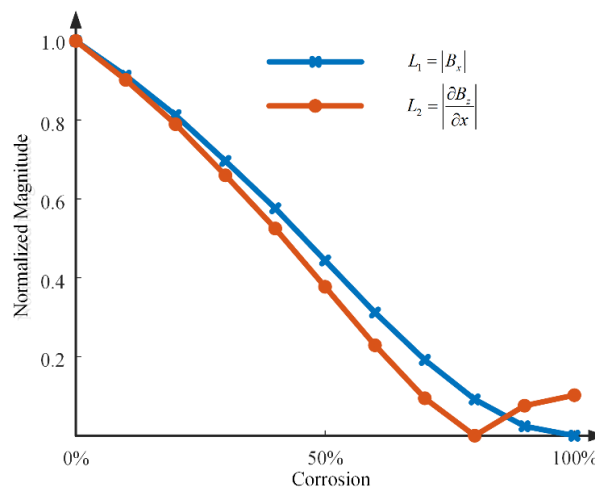
Fig.7 Signal size at different corrosion levels

B. *Effect of sensor attitude on corrosion detection*

In the case of sensor attitude change, the signal values Bx and Bz at x=5.0m will be more noisy with the attitude angle, which will make the calculation of the signal values |Bx| and |∂Bz/∂x| deviate. In order to analyze the effect of attitude angle on the corrosion degree, the maximum attitude angles of 10º, 20º and 30º are considered respectively, and the corrosion degree at the attitude angle is calculated using the correspondence shown in Fig.7, and the attitude effect is evaluated using the error rate E.

$$E = |f_1 - f_0| \times 100\% \qquad (5)$$

In the above equation f1 is the calculated corrosion degree under the considered attitude angle and f0 is the corrosion degree under the standard attitude

The correspondence of sensor attitude to corrosion degree error is shown in Fig.8. For the signal value |Bx|, the detection error rate at the same degree of corrosion increases with the maximum attitude angle. This is because an increase in the attitude angle leads to an increase in the signal value error, which leads to an increase in the error rate; the increase in the detection error corrosion rate at the same attitude angle decreases first and

then increases. This is because under the influence of the attitude angle, the proportion of noise in the signal generated by the attitude angle decreases first and then increases. For the signal value $|\partial Bz/\partial x|$, the relationship between the detection error rate at the same corrosion degree and the maximum attitude angle is not linear, which is due to the fact that it is difficult to obtain the accurate value of the slope calculation of its Bz component under the consideration of the noise, and its calculated value will be largely affected by the noise and produce unpredictable errors.
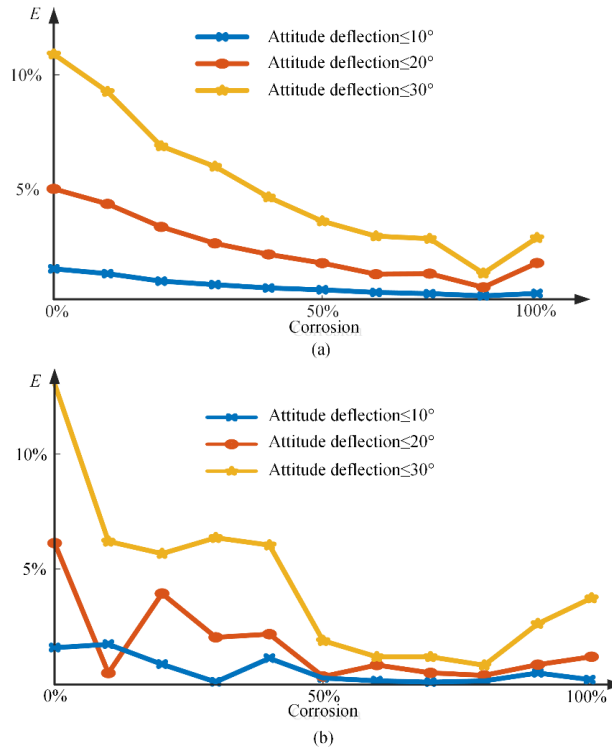
Fig. 8 Calculation errors of different attitude deflections on corrosion degree

(a) Bx (b) $\partial Bz/\partial x$

C. Detection Optimization

The single-component sensor measurement system is prone to lose the original magnetic field information due to attitude deflection during the detection process, and this information loss is not reversible, that is, it cannot be simply corrected by the recorded attitude angle. Aiming at the analysis of the sensor attitude on the detection error of the grounding network state, this paper proposes an optimization scheme of attitude correction to improve the accuracy of the grounding grid state evaluation.

The magnetic field vector sum induced by the three-component quadrature sensor system in the measurement process is not changed by the change of the sensor attitude. By adding the attitude angle measurement to the three-component quadrature sensor system, the Bx, By, and Bz components when the attitude angle is zero are re-extracted based on the information of the attitude angle, and then the calculation of the topology or corrosion degree of the grounding grid is carried out, so as to realize the accurate measurement of the state of the grounding grid, and the process is shown in Fig.9.
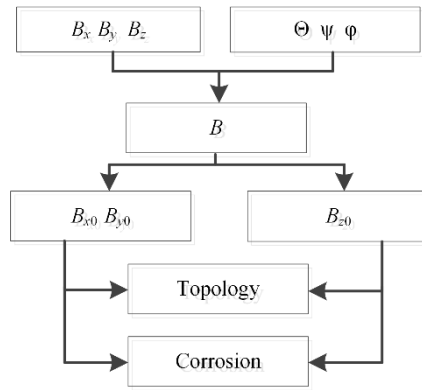
Fig.9 Optimize the detection process

IV. DISCUSSION

For the surface magnetic field method in the actual grounding grid state detection will encounter measurement problems, this paper through the maximum attitude angle to simulate the attitude deflection state in the field detection, the detection process of the sensor attitude changes brought about by the measurement error was analyzed to optimize the detection scheme, there are the following findings:

(1) The sensor attitude can have an effect on the measurement signal causing the signal amplitude or slope to be difficult to calculate, thus affecting the identification of the grounding grid topology. The single-component magnetic field measurement device should try to ensure that its attitude is not deflected to ensure the accuracy of the signal.

(2) In the measurement process, the sensor attitude changes will affect the calculation of the degree of corrosion of the grounding grid, for the signal |Bx|, the actual degree of corrosion of the ground grid will make its calculation error is the first to reduce and then increase, and the same state of the ground grid, the larger the attitude deflection, the larger the error rate of the calculation; for the signal $|\partial Bz/\partial x|$ for the direction of the measurement line of the slope of Bz is difficult to calculate the accuracy of the direction of the line of measurement and lead to its corrosion without a fixed law for the degree error rate.

(3) The accuracy of the detection system can be improved by recalculating the horizontal component magnetic field or vertical component magnetic field by the three-component sensor device and attitude measurement to reduce the error brought by the sensor attitude deflection to the single-component magnetic field signal.

REFERENCE

[1] H. Lin et al., "Evaluation and optimization of safety performance state of grounding grid," 2021 IEEE 4th International Electrical and Energy Conference (CIEEC), Wuhan, China, 2021, 1-4, DOI: 10.1109/CIEEC50170.2021.9510929.

[2] W. Xuming et al., "Analysis of Safety Index in Substation Considering the Damage of External Ground Network," 2022 IEEE 6th Conference on Energy Internet and Energy System Integration (EI2), Chengdu, China, 2022, 658-663, DOI: 10.1109/EI256261.2022.10116108.

[3] Y. Zhang et al., "Impact of Grid Topology on Pole-to-ground Fault Current in Bipolar DC Grids: Mechanism and Evaluation," in Journal of Modern Power Systems and Clean Energy, 2023, 11(2): 434-445, DOI: 10.35833/MPCE.2021.000399.

[4] N. Permal, M. Osman, A. M. Ariffin and M. Z. A. A. Kadir, "The Impact of Substation Grounding Grid Design Parameters in Non-Homogenous Soil to the Grid Safety Threshold Parameters," in IEEE Access, 2021(9): 37497-37509, DOI: 10.1109/ACCESS.2021.3063018.

[5] B. M. Samy, I. I. I. Mansy and E. A. Badran, "On the Transient Voltages of Grounding Grids," 2023 24th International Middle East Power System Conference (MEPCON), Mansoura, Egypt, 2023: 1-6, DOI: 10.1109/MEPCON58725.2023.10462458.

[6] N. Zhou, S. C. Zhang, X. M. Wang, "Comprehensive Safety Check Analysis of Substation Grounding Grid," Insulators and Surge Arresters, 2021(03): 119-124. DOI: 10.16188/j.isa.1003-8337.2021.03.018.

[7] Y. Dan, Z. Zhang, P. Gan, H. Ye, Q. Li and J. Deng, "Performance Analysis of Corroded Grounding Devices with an Accurate Corrosion Model," in CSEE Journal of Power and Energy Systems, 2023, 9(3): 1235-1247, DOI: 10.17775/CSEEJPES.2020.03280.

[8] X. Wang, J. Yong and W. Xu, "An Online Method for Monitoring Substation Grounding Grid Impedances—Part II: Verifications and Applications," in IEEE Transactions on Power Delivery, 2022, 37(4): 2533-2542, DOI: 10.1109/TPWRD.2021.3112073.

[9] Z. Liu and B. Zhang, "Test Method for Transient Characteristics of Grounding Grid With Current Return Point Located in the Same Grid," in IEEE Transactions on Power Delivery, 2022, 37(4): 2902-2910, DOI: 10.1109/TPWRD.2021.3119184.

[10] Z. Zhang, H. Ye, Y. Dan, Z. Duanmu, Y. Li and J. Deng, "Novel Method for Comprehensive Corrosion Evaluation of Grounding Device," in IEEE Access, 2020(8): 72102-72111, DOI: 10.1109/ACCESS.2020.2985534.

[11] Z. Zhou, G. Ma, B. Liu, X. Chu and S. Yu, "Research on Fault Diagnosis Method of Grounding Grid Based on WDA-uVOL," 2023 3rd New Energy and Energy Storage System Control Summit Forum (NEESSC), Mianyang, China, 2023, 206-209, DOI: 10.1109/NEESSC59976.2023.10349273.

[12] C. Lu et al., "Fault Diagnosis of Tower Grounding Conductor Based on the Electromagnetic Measurement and Neural Network," in IEEE Transactions on Instrumentation and Measurement, 2022, 71: 1-9, DOI: 10.1109/TIM.2022.3192070.

[13] X. Zhang, B. Yu, L. Liu, Z. Fu, J. Yu and X. Cheng, "Accumulative Imaging Method of Grounding Grid Topological Features Based on Combined Sources," in IEEE Access, 2024, 12: 60876-60882, DOI: 10.1109/ACCESS.2024.3394688.

[14] S. L. Zhang, D. L. Liu, H. F. Xu, W. L. Song, L. Wang, "Detection and Evaluation Method of Breakpoint and Corrosion Magnetic Field of Substation Grounding Grid," Insulators and Surge Arresters, 2020(05): 190-193. DOI: 10.16188/j.isa.1003-8337.2020.05.031.

[15] S. L. Zhang, D. L. Liu, H. F. Xu, W. L. Song, Z. H. Pan, Y. Liu, X. Guo, "Detection Method of Corrosion Brakpoint of Grounding Grid Based on Distribution Characteristics of Magnetic Field," Insulators and Surge Arresters, 2021(01): 51-55+62. DOI: 10.16188/j.isa.1003-8337.2021.01.008.

[16] X. Y. Wang, W. He, F. Yang, L. W. Zhu, X. P. Liu, "Topology Detection of Grounding Grids Based on Derivative Method," Transactions of China Electrotechnical Society, 2015, 30(03): 73-78+89. DOI: 10.19595/j.cnki.1000-6753.tces.2015.03.010.

[17] Z. Fu, S. Song, X. Wang, J. Li and H. -M. Tai, "Imaging the Topology of Grounding Grids Based on Wavelet Edge Detection," in IEEE Transactions on Magnetics, 2018, 54(4): 1-8, DOI: 10.1109/TMAG.2018.2791565.

[18] Y. Xie, X. Fan, H. Chen, X. Li and Y. Tang, "Method of grounding grid detection signal filtering," 2022 2nd International Signal Processing, Communications and Engineering Management Conference (ISPCEM), Montreal, ON, Canada, 2022: 324-328, DOI: 10.1109/ISPCEM57418.2022.00071.